

Tuning the Structure and Magnetism of Azido-Mediated Cu^{II} Systems by Coligand Modifications

Jiong-Peng Zhao,[†] Bo-Wen Hu,[†] E. C. Sañudo,[‡] Qian Yang,[†] Yong-Fei Zeng,[†] and Xian-He Bu^{*†}

Department of Chemistry, Nankai University, Tianjin 300071, P. R. China, and Departament de Química Inorgànica, Universitat de Barcelona, Diagonal, 647, 08028-Barcelona, Spain

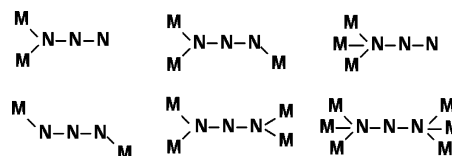
Received October 27, 2008

Through the use of a series of structurally related benzoates bearing different substituents as coligands, three new azido–copper compounds, [Cu(benzoate)(N₃)_n] (1), [Cu(2-methyl-benzoate)(N₃)_n] (2), and [Cu(1-naphthoate)(N₃)_n] (3), have been successfully obtained and structurally and magnetically characterized. Single-crystal structure analyses indicated that the uncoordinating substituents in the benzoates greatly affect the structure of the complexes. Complex 1 displays isolated ferromagnetic chains with the largest Cu–N–Cu angle in known carboxylate/end-on-azido mixed-bridged copper systems, while complexes 2 and 3 were 2D coordination polymers, containing μ-(1,1,3,3) and μ-(1,1,3) bridging azides and exhibiting new azido–copper networks with (4⁴) and (4 · 8²) topologies, respectively. Furthermore, 2 was a chiral complex obtained through spontaneous resolution. In the low-temperature range, both 2 and 3 showed spontaneous magnetization with characteristics of soft ferromagnetic magnetism with phase transition temperatures of 13 and 10 K, respectively.

Introduction

The azido ligand is able to link metal ions in different coordination modes, which induces rich structural diversity as well as a range of different magnetic properties in the azido–metal complexes.^{1–6} The azido-based Cu^{II} coordination polymers are among the most important kinds of

Chart 1



azido–metal complexes.^{7,8} End-on (EO) and end-to-end (EE) are two typical bridging modes for the azido linker in azido–metal systems, but the azido ligand can bridge more than two metals in a combination of EE and EO modes (Chart 1). All of the bridging modes can be symmetric or asymmetric and with or without the presence of col-

* To whom correspondence should be addressed. Fax: +86-22-23502458. Tel: +86-22-23502809. E-mail: buxh@nankai.edu.cn.

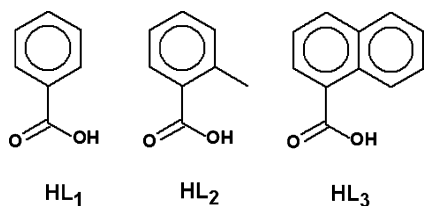
[†] Nankai University.

[‡] Universitat de Barcelona.

- (1) Kahn, O. *Molecular Magnetism*; VCH: New York, 1993.
- (2) For example: (a) Ribas, J.; Escuer, A.; Monfort, M.; Vicente, R.; Cortes, R.; Lezama, L.; Rojo, T. *Coord. Chem. Rev.* **1999**, *193–195*, 1027. (b) Zeng, Y.-F.; Hu, X.; Liu, F.-C.; Bu, X.-H. *Chem. Soc. Rev.* **2009**, *38*, 469.
- (3) For example: (a) Hong, C. S.; Do, Y. *Angew. Chem., Int. Ed.* **1999**, *38*, 193. (b) Maji, T. K.; Mukherjee, P. S.; Mostafa, G.; Mallah, T.; Cano-Boquera, J.; Chaudhuri, N. R. *Chem. Commun.* **2001**, 1012. (c) Liu, T.-F.; Fu, D.; Gao, S.; Zhang, Y.-Z.; Sun, H.-L.; Su, G.; Liu, Y.-J. *J. Am. Chem. Soc.* **2003**, *125*, 13976.
- (4) Gao, E.-Q.; Bai, S.-Q.; Wang, Z.-M.; Yan, C.-H. *J. Am. Chem. Soc.* **2003**, *125*, 4984.
- (5) For example: (a) Yoo, H. S.; J, Kim, I.; Yang, N.; Koh, E. K.; Park, J. G.; Hong, C. S. *Inorg. Chem.* **2007**, *46*, 9054. (b) Biani, F. F.; Ruiz, E.; Cano, J.; Novoa, J. J.; Alvarez, S. *Inorg. Chem.* **2000**, *39*, 3221. (c) Escuer, A.; Aroms, G. *Eur. J. Inorg. Chem.* **2006**, 4721.
- (6) For example: (a) Abu-Youssef, M. A. M.; Escuer, A.; Langer, V. *Eur. J. Inorg. Chem.* **2006**, *45*, 3177. (b) Abu-Youssef, M. A. M.; Drillon, M.; Escuer, A.; Goher, M. A. S.; Mautner, F. A.; Vicente, R. *Inorg. Chem.* **2000**, *39*, 5022.

- (7) For example: (a) Guo, G.-C.; Mak, T. C. W. *Angew. Chem., Int. Ed.* **1998**, *37*, 3286. (b) Goher, M. A. S.; Cano, J.; Journaux, Y.; Abu-Youssef, M. A. M.; Mautner, F.; Escuer, A.; Vicente, R. *Chem.—Eur. J.* **2000**, *6*, 778. (c) Villanueva, M.; Mesa, J. L.; Urriaga, M. K.; Cortes, R.; Lezama, L.; Arriortua, M. I.; Rojo, T. *Eur. J. Inorg. Chem.* **2001**, *61*, 1581. (d) Maji, T. K.; Mukherjee, P. S.; Koner, S.; Mostafa, G.; Tuchagues, J.-P.; Chaudhuri, N. R. *Inorg. Chim. Acta* **2001**, *314*, 111.
- (8) (a) Meyer, F.; Kircher, P.; Pritzkow, H. *Chem. Commun.* **2003**, 774. (b) Escuer, A.; Vicente, R.; Fallah, M. S. E.; Goher, M. A. S.; Mautner, F. A. *Inorg. Chem.* **1998**, *37*, 4466. (c) Barone, A. C.; Bencini, V.; Bencini, A.; Totti, F.; Ciofini, I. *Inorg. Chem.* **1999**, *38*, 1996.
- (9) (a) Mondal, K. C.; Mukherjee, P. S. *Inorg. Chem.* **2008**, *47*, 4215. (b) Stamatatos, T. C.; Papaefstathiou, G. S.; MacGillivray, L. R.; Escuer, A.; Vicente, R.; Ruiz, E.; Perlepes, S. P. *Inorg. Chem.* **2007**, *46*, 8843. (c) Liu, T.; Yang, Y.-F.; Wang, Z.-M.; Gao, S. *Chem. Asian J.* **2008**, *3*, 950.

Chart 2



gands.^{9–11} It is well-established that the EE modes usually propagate antiferromagnetic while the EO modes are usually ferromagnetic, although the coupling between metal ions bridged by EO azido ligands can be antiferromagnetic in the presence of other bridging ligands or for very large metal–N–metal angles.¹² Several structural parameters, especially the Cu–N–Cu angle, affect the superexchange mechanism.^{13,14} Modifying the coligand would also influence the geometry of the azido–metal moiety and would thus have an effect on the magnetic properties of the complexes.²

Although azido can mediate strong coupling between Cu^{II} ions, there are still few examples that exhibit long-range ordering phenomena.¹⁵ The common strategy for the enhancement of bulk magnetic properties is introducing a second neutral organic linker such as amine, bipyridine, or bisimidazole.¹⁶ Recently, three-dimensional (3D) azido–metal complexes were reported by employing a negatively charged pyridyl carboxylate as a coligand, which resulted in a novel topology of the materials and enhancement of the bulk magnetic properties of the azido–metal systems, with some of them exhibiting ferromagnetic ordering.^{15a,17} In this work, we investigate the use of benzoate and substituted benzoates (Chart 2) as coligands to azido–Cu complex systems. With this modification in the coligand substituents, we expect to be able to tune the structure and magnetic properties of the resulting azido–Cu systems.

Herein, we report the synthesis, structural characterization, and magnetic properties of three new azido–Cu coordination polymers, [Cu(L₁)(N₃)_n] (1), [Cu(L₂)(N₃)_n] (2), and [Cu(L₃)(N₃)_n] (3). Interestingly, our results indicate that altering the substitutional groups of coligands greatly influences the structure of the resulting complexes, which in turn results in different magnetic behaviors. Complex 1 consists of isolated one-dimensional (1D) ferromagnetic chains with a large Cu–N–Cu angle of 126.8°, which to the best of our knowledge is the largest in known carboxylate/EO-azido mixed-bridged copper compounds,^{17a} while 2 and 3 are two-dimensional (2D) ferromagnetic networks exhibiting new azido–copper structures with (4⁴) and (4·8²) topology, respectively. Additionally, complex 2 is a chiral complex obtained through spontaneous resolution.

Experimental Section

Materials. All of the chemicals used for synthesis are of analytical grade and are commercially available. Cu(NO₃)₃·3H₂O, sodium hydroxide, sodium benzoate, 2-methyl-benzoic acid, α-naphthalic acid, and sodium azide were purchased from commercial sources and used as received.

Caution! Azide–metal complexes are potentially explosive; only a small amount of material should be prepared and with care.

Physical Measurements. Elemental analyses (C, H, N) were performed on a Heraeus CHN-Rapid elemental analyzer (at Institute of Chemistry, CAS). IR spectra were measured on a Tensor 27 OPUS (Bruker) FT-IR spectrometer with KBr pellets. The X-ray powder diffraction (XRPD) was recorded on a Rigaku D/Max-2500 diffractometer at 40 kV and 100 mA using a Cu-target tube and a graphite monochromator. Simulation of the XRPD spectra was carried out using the single-crystal data and diffraction-crystal module of the Mercury (Hg) program, available free of charge via the Internet at <http://www.iucr.org>.

Magnetic data were collected using crushed crystals of the sample on a Quantum Design MPMS-XL SQUID magnetometer equipped with a 5T magnet. The data were corrected using Pascal's constants to calculate the diamagnetic susceptibility, and an experimental correction for the sample holder was applied.

Synthesis. Single crystals of complexes 1–3 suitable for X-ray analysis were obtained using a method similar to that described below for 1, except 2-methyl-benzoic acid and α-naphthalic acid were used instead of sodium benzoate for 2 and 3, respectively, while NaOH in this procedure was in a slight excess (1 mmol).

[Cu(benzoate)(N₃)_n] (1). Complex 1 was hydrothermally synthesized under autogenous pressure. A mixture of Cu(NO₃)₃·3H₂O (1 mmol), sodium benzoate (0.4 mmol), NaOH (0.5 mmol), NaN₃ (1.5 mmol), and H₂O (10 mL) was sealed in a Teflon-lined autoclave and heated to 140 °C. After being maintained for 48 h, the reaction vessel was cooled to room temperature over 12 h. Pure green-black crystals were collected. Yield: ~20% based on Cu(NO₃)₃·3H₂O. FT-IR (KBr pellets, cm⁻¹): 3132, 2096, 1589, 1534, 1401, 1266, 723, 684. Anal. calcd for C₇H₅CuN₃O₂: C, 37.09; H, 2.22; N, 18.54%. Found: C, 37.35; H, 2.31; N, 18.01%.

Synthesis of [Cu(2-methyl-benzoate)(N₃)_n] (2). Yield: ~30%. FT-IR (KBr pellets, cm⁻¹): 3415, 3134, 2080, 1617, 1527, 1401, 1125, 738, 618. Anal. calcd for C₈H₇CuN₃O₂: C, 39.92; H, 2.93; N, 17.46%. Found: C, 39.50; H, 2.90; N, 16.74%.

Synthesis of [Cu(1-naphthoate)(N₃)_n] (3). Yield: ~20%. FT-IR (KBr pellets, cm⁻¹): 3130, 2086, 1595, 1515, 1460, 1402, 1288, 798, 788, 776, 659, 595, 542, 507, 481, 417. Anal. calcd for

- (10) (a) Tangoulis, V.; Panagoulis, D.; Raptopoulou, C. P.; Samara, C. D. *Dalton Trans.* **2008**, 1752. (b) Han, Y.-F.; Wang, T.-W.; Song, Y.; Shen, Z.; You, X.-Z. *Inorg. Chem. Commun.* **2008**, *11*, 207. (c) Feng, P. L.; Beedle, C. C.; Wernsdorfer, W.; Koo, C.; Nakano, M.; Hill, S.; Hendrickson, D. N. *Inorg. Chem.* **2007**, *46*, 8126.
- (11) (a) Chen, H.-J.; Mao, Z.-W.; Gao, S.; Chen, X.-M. *Chem. Commun.* **2001**, 2320. (b) Woodard, B.; Willett, R. D.; Haddad, S.; Twamley, B.; Garcia, C. J.; Coronado, E. *Inorg. Chem.* **2004**, *43*, 8126.
- (12) (a) Kahn, O.; Sikorav, S.; Gouteron, J.; Jeannin, S.; Jeannin, Y. *Inorg. Chem.* **1983**, *22*, 2877. (b) Cortes, R.; Urtiaga, M. K.; Lezama, L.; Larramendi, J. I. R.; Arriortua, M. I.; Rojo, T. J. *Chem. Soc., Dalton Trans.* **1993**, 3685. (c) Thompson, L. K.; Tandon, S.S. *Comments Inorg. Chem.* **1996**, *18*, 125. (d) Zhang, L.; Zuo, J.-L.; Gao, S.; Song, Y.; Che, C.-M.; Fun, H.-K.; You, X.-Z. *Angew. Chem., Int. Ed.* **2000**, *39*, 3633.
- (13) (a) Ruiz, E.; Cano, J.; Alvarez, S.; Alemany, P. *J. Am. Chem. Soc.* **1998**, *120*, 11122. (b) Cabrero, J.; Graaf, C.; Bordas, Caballol, E.; R.; Malrieu, J.-P. *Chem.—Eur. J.* **2003**, *9*, 2307. (c) Triki, S.; Garcia, C. J. G.; Ruiz, E.; Pala, J. S. *Inorg. Chem.* **2005**, *44*, 5501.
- (14) (a) Mialane, P.; Dolbecq, A.; Marrot, J.; Rivière, E.; Sécheresse, F. *Chem.—Eur. J.* **2005**, *11*, 1771. (b) Nanda, P. K.; Aromi, G.; Ray, D. *Chem. Commun.* **2006**, 3181.
- (15) (a) Zeng, Y.-F.; Liu, F.-C.; Zhao, J.-P.; Cai, S.; Bu, X.-H.; Ribas, J. *Chem. Commun.* **2006**, 2227. (b) Gu, Z.-G.; Song, Y.; Zuo, J.-L.; You, X.-Z. *Inorg. Chem.* **2007**, *46*, 9522. (c) Gu, Z.-G.; Zuo, J.-L.; You, X.-Z. *Dalton Trans.* **2007**, 4067.
- (16) Gao, E.-Q.; Wang, Z.-M.; Yan, C.-H. *Chem. Commun.* **2003**, 1748. (b) Wang, X.-Y.; Wang, L.; Wang, Z.-M.; Gao, S. *J. Am. Chem. Soc.* **2006**, *128*, 674. (c) Wang, X. Y.; Wang, Z. M.; Gao, S. *Chem. Commun.* **2008**, 281.
- (17) (a) He, Z.; Wang, Z.-M.; Gao, S.; Yan, C.-H. *Inorg. Chem.* **2006**, *45*, 6694. (b) Zeng, Y.-F.; Zhao, J.-P.; Hu, B.-W.; Hu, X.; Liu, F.-C.; Ribas, J.; Ribas-Ariño, J.; Bu, X.-H. *Chem.—Eur. J.* **2007**, *13*, 9924.

Table 1. Crystal Data and Structure Refinement Parameters for Complexes **1–3**

	1	2	3
chemical formula	C ₇ H ₅ CuN ₃ O ₂	C ₈ H ₅ CuN ₃ O ₂	C ₁₁ H ₅ CuN ₃ O ₂
fw	226.68	240.71	276.74
space group	<i>Pnma</i>	<i>P2(1)2(1)2(1)</i>	<i>P2(1)/c</i>
<i>a</i> (Å)	6.8436(14)	4.9590(10)	15.912(12)
<i>b</i> (Å)	7.0732(14)	6.4582(13)	6.799(5)
<i>c</i> (Å)	6.600(3)	27.249(5)	9.948(7)
β /deg	90	90	101.981(11)
<i>V</i> /Å ³	803.6(3)	872.7(3)	1052.7(13)
<i>Z</i>	4	4	4
<i>D</i> /g cm ⁻³	1.874	1.832	1.746
μ /mm ⁻¹	2.682	2.475	2.065
<i>T</i>	293	293	293
<i>R</i> ^a / <i>wR</i> ^b	0.1049/0.2586	0.0481/0.0951	0.1026/0.2717

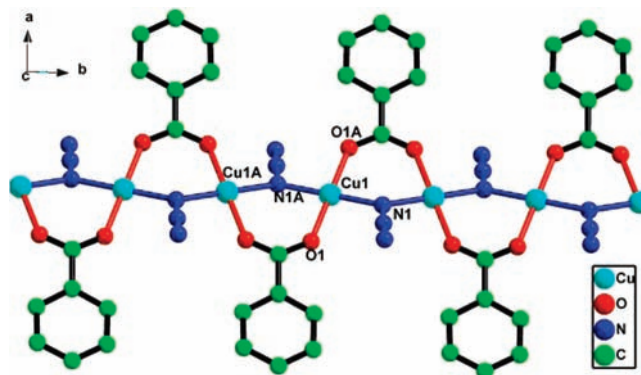
^a $R = \sum ||F_o| - |F_c|| / \sum |F_o|$. ^b $R_w = [\sum w(F_o^2 - F_c^2)^2 / \sum w(F_o^2)]^{1/2}$.

C₁₁H₇CuN₃O₂: C, 47.74; H, 2.55; N, 15.18%. Found: C, 47.77; H, 2.62; N, 15.20%.

X-Ray Data Collection and Structure Determinations. X-ray single-crystal diffraction data for complexes **1–3** were collected on a Bruker Smart 1000 CCD diffractometer at 293(2) K with Mo K α radiation ($\lambda = 0.71073$ Å) in the ω scan mode. The program SAINT¹⁸ was used for integration of the diffraction profiles. All of the structures were solved using direct methods using the SHELXS program of the SHELXTL package and refined using full-matrix least-squares methods with SHELXL (semiempirical absorption corrections were applied using the SADABS program).¹⁹ Metal atoms in each complex were located from the *E*-maps, and other non-hydrogen atoms were located in successive difference Fourier syntheses and refined with anisotropic thermal parameters on *F*². The hydrogen atoms of the ligands were generated theoretically onto the specific atoms and refined isotropically with fixed thermal factors. Detailed crystallographic data are summarized in Table 1.

Results and Discussion

Crystal Structure of the Complexes. The single-crystal X-ray determination reveal that **1** consists of an isolated 1D azido-copper chain. The asymmetric unit of this complex consists of half a Cu^{II} ion, half an azide anion, and half a benzoate ligand. The Cu^{II} ion located at the inverse center takes a square-planar environment coordinated by two nitrogen atoms from two azide anions and two oxygen atoms from two carboxylates [Cu1–N1 = 1.977 Å, Cu1–O1 = 1.954 Å, Cu1–N1A = 1.977 Å, and Cu1–O1A = 1.954 Å]. The azido takes the EO mode linking two Cu^{II} ions, while the carboxylate bridges two Cu^{II} ions together with the azido anions forming a carboxylate/EO-azido mixed-bridged copper chain (Figure 1). In the chain, Cu^{II} ions and the benzoate ligands are almost in one plane. The chains take the ABAB packing mode in the lattice. The Cu1...Cu1A distance is 3.537 Å, while the Cu1–N1–Cu1A angle is 126.8°. It is noticeable that both the copper–copper separation and the μ -(1,1)-N₃ bridge angle are greater than the previously reported examples containing μ -(1,3)-carboxylate/ μ -(1,1)-N₃

**Figure 1.** The 1D carboxylate/EO azido mixed-bridged copper chain of **1**.

mixed-bridged copper compounds.^{10a,15a,17a,21} The nearest separation of Cu^{II} ions between two neighbor chains is 6.844 Å. The key bond distances and angles are listed in Table 2.

In the structure of complex **2**, the 2-methyl-benzoate replaces the benzoate ligand, and different from **1**, the Cu^{II} ion is hexacoordinated with tetragonal axial elongation. Two nitrogen atoms and two oxygen atoms coordinated to the Cu^{II} ion in the equatorial plane [Cu1–N1 = 1.986 Å, Cu1–N1A = 2.003 Å, Cu1–O1 = 1.932 Å, and Cu1–O2A = 1.918 Å], while the axial is taken by two azido anions [Cu1–N3A = 2.604 Å and Cu1–N3B = 2.695 Å]. The carboxylate group bridges two Cu^{II} ions adopting the *syn,syn* mode. There is a 32.0° torsion of the carboxylate group from the benzene ring. The azido ions are in the μ -(1,1,3,3) bridging mode, using one end to coordinate to two Cu^{II} ions on the equatorial plane while the other end links to one Cu^{II} ion using its apical position of the square-based pyramid (Figure 2a). The distances of Cu^{II} ions linked by azido in the EO mode are 3.230 Å, while the EE modes are 4.959 Å and 5.956 Å in the *cis* and *trans* forms, respectively. The Cu–N–Cu angles are 108.16° in the equatorial plane and 75.09° in the axial positions. The Cu1–N1–N2 and Cu1A–N1–N2 angles are 118.3° and 117.2°, while the angles Cu1G–N3–N2 and Cu1G–N3–N2 are 109.4° and 110.5°, respectively. The structure of **2** can be easily described as well-isolated layers of hexacoordinated Cu^{II} ions along the *ab* plane of the unit cell; each Cu^{II} center exhibits a tetragonal axial elongation, in which the unpaired electron is on the $d_{x^2-y^2}$ orbital (the two elongated Cu–N distances are 2.695 and 2.604 Å, respectively). Each layer is formed by the chains of Cu^{II} ions bridged by an EO azido and a *syn,syn*-carboxylate group, and these chains are in turn linked to form the 2D layer by end-to-end azido ligands. The layers are magnetically isolated from each other, with Cu–Cu distances of 14 Å. It is interesting that both the azido groups and Cu^{II} ions in the 2D layer can be considered to be 4-connected nodes; thus, the 2D network can be described as having (4⁴) topology constructed by azido and copper (Figure 3).

For **2**, the methyl substitutional groups of the coligand affect not only the linkage of azido anions but also the

(18) SAINT Software Reference Manual; Bruker AXS: Madison, WI, 1998.
 (19) Sheldrick, G. M. SHELXTL NT, version 5.1; University of Göttingen: Göttingen, Germany, 1997.

(20) Thompson, L. K.; Tandon, S. S.; Lloret, F.; Cano, J.; Julve, M. *Inorg. Chem.* **1997**, *36*, 3301.

(21) Escuer, A.; Vicente, R.; Mautner, F. A.; Goher, M. A. S. *Inorg. Chem.* **1997**, *36*, 1233.

Table 2. Selected Bond Lengths [Å] and Angles for **1–3** [deg]

		1		
Cu(1)–O(1)#1	1.954(6)		Cu(1)#2–N(1)–Cu(1)	126.8(6)
Cu(1)–O(1)	1.954(6)		O(1)–Cu(1)–N(1)	91.2(4)
Cu(1)–N(1)#1	1.978(5)		N(1)#1–Cu(1)–N(1)	180.0(7)
Cu(1)–N(1)	1.978(5)		O(1)#1–Cu(1)–O(1)	180.0(4)
#1–x + 1, –y, –z + 1	#2–x + 1, y + 1/2, –z + 1			
		2		
Cu(1)–O(2)#1	1.919(4)		Cu(1)#4–N(1)–Cu(1)	108.16(19)
Cu(1)–O(1)	1.932(3)		Cu(1)#5–N(3)–Cu(1)#6	75.09(13)
Cu(1)–N(1)#1	1.986(4)		N(1)–Cu(1)–N(3)#2	85.69(16)
Cu(1)–N(1)	2.003(4)		N(1)#1–Cu(1)–N(3)#2	94.28(16)
Cu(1)–N(3)#2	2.604(5)		O(2)#1–Cu(1)–N(1)#1	90.20(16)
Cu(1)–N(3)#3	2.695(5)		O(1)–Cu(1)–N(1)#1	89.99(16)
#1–x + 2, y–1/2, –z + 1/2	#2x–1, y, z		#3–x + 3, y–1/2, –z + 1/2	#4–x + 2, y + 1/2, –z + 1/2
#5x + 1, y, z	#6–x + 3, y + 1/2, –z + 1/2			
		3		
Cu(1)–O(2)#1	1.932(9)		Cu(1)–N(1)–Cu(1)#1	116.8(5)
Cu(1)–O(1)	1.932(9)		N(2)–N(3)–Cu(1)#3	111.3(10)
Cu(1)–N(1)	1.987(10)		O(2)#1–Cu(1)–N(1)	91.0(4)
Cu(1)–N(1)#2	2.014(10)		O(1)–Cu(1)–N(1)	91.8(4)
Cu(1)–N(3)#3	2.726(13)		N(1)–Cu(1)–N(3)#3	88.8(4)
#1–x + 2, y–1/2, –z + 3/2	#2–x + 2, y + 1/2, –z + 1/2		#3–x + 2, –y, –z + 1	

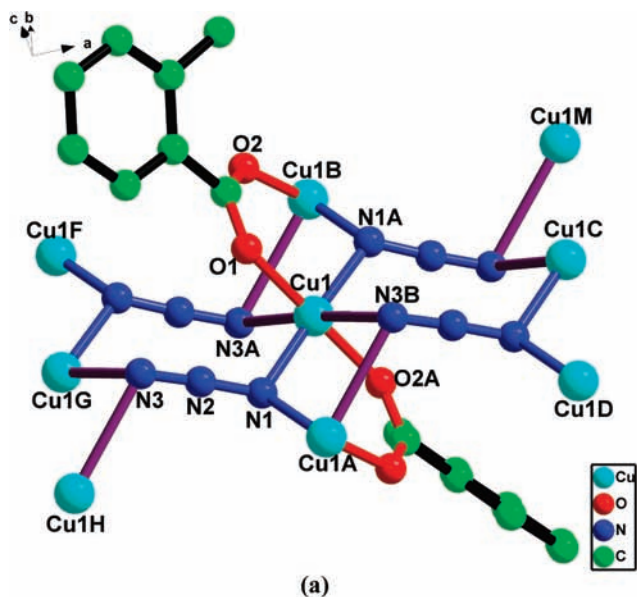
conformation of the layers compared to **1**, which results in the chiral structure of the complex obtained through spontaneous resolution. When coordinated to the metal ions, the methyl groups of the 2-methyl-benzoates all point along the *b* axis deviated from the phenyl, and the phenyl groups at the topside and the underside of the copper–azido layer have a dihedral angle of 64.05°. Although the azido and the coligand 2-methyl-benzoate are all achiral, in the process of crystallization, a chiral layer was formed. When the layers pack to high dimension, the layers are related by a 2-fold screw axis. Hence, such sheets stack along the *c* axis, forming a chiral crystal of **2**, and spontaneous resolution occurs with a generated conglomerate. The Flack parameter of **2** is 0.14(5); thus, the absolute structure cannot be determined.

It is interesting that, although the steric bulk of the side group of coligand carboxylate becomes larger gradually in **1**, **2**, and **3**, the structure of **3** can be considered as the integration of **1** and **2**. Different from **1** and **2**, the Cu^{II} ions in **3** were pentacoordinated [Cu1–N1 = 1.987 Å, Cu1–N1B = 2.014 Å, Cu1–O1 = 1.933 Å, Cu1–O2A = 1.932 Å, and Cu1–N3A = 2.726 Å] (Figure 2b). The angle between the carboxylate group and naphthalene ring is 40°. The carboxylate group bridges two Cu^{II} ions with the *syn,syn* mode. The azido anion of **3** takes the μ -(1,1,3) mode coordinating to Cu^{II} ions in the equatorial plane, giving a carboxylate/EO-azido mixed-bridged copper chain like **1** and **2**; then, the chains are linked by μ -(1,1,3)-N₃, forming a 2D net. The Cu–N–Cu angle is 116.8°, and the Cu1D–N3–N2 bond angle is 111.3°. The distances of Cu^{II} ions bridged by the same azido anion are 3.409, 5.493, and 5.118 Å. In **3**, the azide and Cu^{II} are only connected to three of each other. The azido–copper net could be described as (4·8²) topology (Figure 3). The key bond distances and the angles are listed in Table 2. It is worth noting that the uncoordinating substitutional groups of carboxylate in **2** and **3** take a key role in determining the bridge mode of the azido anions. Unlike most other heterocyclic carboxylate or di-carboxylate groups used as coligands in an azido–copper system forming

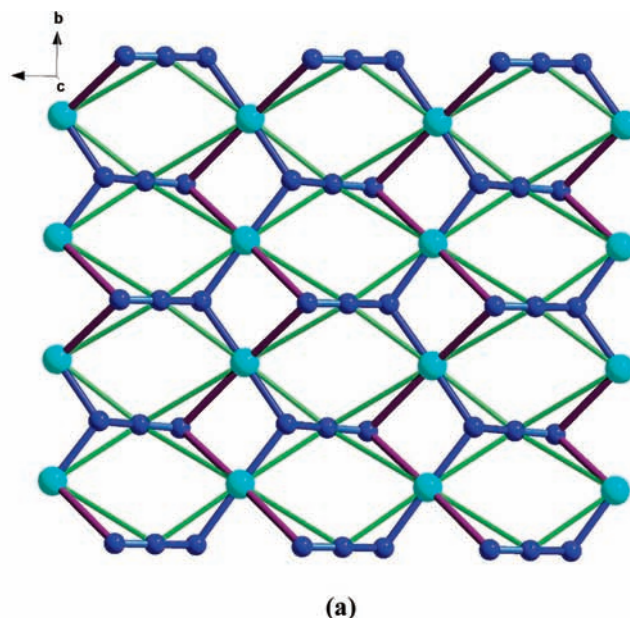
multidimensional complexes via the long bridging coligand, in **2** and **3**, the azido anions link the Cu^{II} ion, forming high-dimensional complexes,^{10a,b,17a,21} which favors interchain magnetic coupling, especially at low temperatures. The layers of **3** are also chiral like that in **2**, but in stacking to high dimension, the neighboring layers are related by a glide plane, making the adjacent layers have opposite handedness. The chirality is annihilated; complex **3** is therefore a racemate in the 3D crystal. The difference in structure between **1**, **2**, and **3** reflected the steric repulsion effect of the coligands. In **1**, without a substituent group on the aryl ring, the azido groups are held very close to the aryl ring, with a small dihedral angle with the plane of the aryl ring. This prevents the azido coordinating to other metal in an end-to-end fashion. For **2** and **3**, with a substituent group on the ligand, the steric repulsions should be stronger. In complex **2**, the substituent is not very large, and thus the azido anions are held apart from the aryl ring, are not very sterically hindered, and can link four metal ions. However, in **3**, the substituent is too bulky, and the azido ligand is too sterically hindered by the substituent of the aryl group to bridge four metal ions.

Magnetic Studies. Magnetic measurements have been carried out on crystalline samples of complexes **1–3**, which were all pure-phase, as confirmed by XRPD (see Figure S1 in the Supporting Information). According to the obtained data, a dominant ferromagnetic coupling between the Cu^{II} ions in **1–3** can be suggested. However, in the low-temperature region, they show various magnetic behaviors, as discussed below.

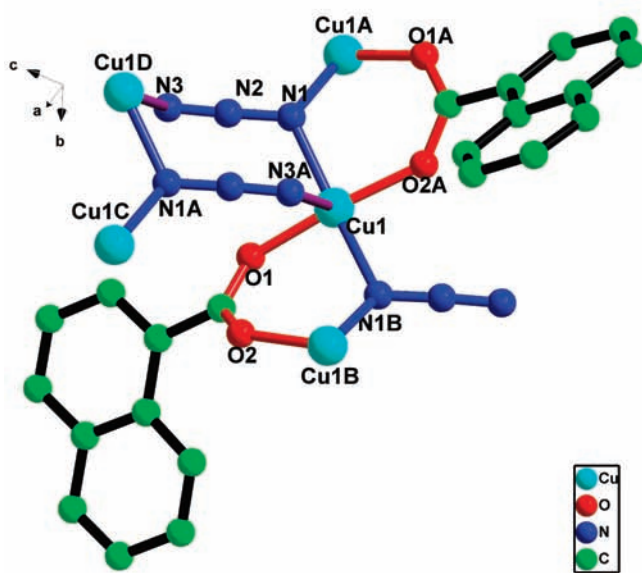
Magnetic susceptibility data of **1** were collected for the crushed crystalline sample of the complex in the 2–300 K temperature range (Figure 4). The $\chi_m T$ value per Cu^{II} ion at 300 K is 0.56 cm³ K mol^{–1}, larger than the predicted 0.375 cm³ K mol^{–1} for an isolated Cu^{II} ion (*S* = 1/2) with *g* = 2.0. As the temperature decreases, the $\chi_m T$ product increases, indicating ferromagnetic coupling between the Cu^{II} ions in **1**. This behavior is not field-dependent. The susceptibility of **1** follows the Weiss law at temperatures above 100 K,



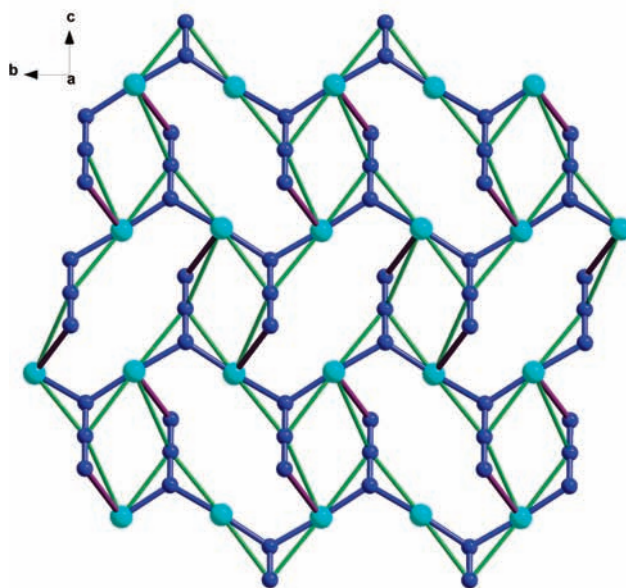
(a)



(a)



(b)



(b)

Figure 2. The linkage and coordination modes for complexes (a) **2** and (b) **3**. Blue bonds stand for equatorial coordination and the dark red for axial.

with $C = 0.504 \text{ emu mol}^{-1}$ and a Weiss constant of $\Theta = 34.62 \text{ K}$, indicating ferromagnetic coupling in **1** (Figure S2, Supporting Information). The experimental data above 10 K can be modeled using Baker's equation for an infinite chain of $S = 1/2$ spins²² based on the Hamiltonian $\hat{H} = -J\sum_i \hat{S}_i \hat{S}_{i+1}$. The best fit, shown in Figure 4 as a solid line, was obtained for $g = 2.28$, $J = 33.90 \text{ cm}^{-1}$, and $R = 3.77 \times 10^{-4}$ ($R = \sum[(\chi_m T)_{\text{obsd}} - (\chi_m T)_{\text{calcd}}]^2 / \sum[(\chi_m T)_{\text{obsd}}]^2$), confirming the strong ferromagnetic coupling between the Cu^{II} centers. Magnetizations versus field data at 2 K were collected for **1** (Figure 4, inset). Magnetization rises very fast as the field increases, indicating ferromagnetic coupling along the Cu^{II} chain, and tends to saturation at the higher fields, as expected for one

(22) Baker, G. A.; Rushbrooke, G. S. *Phys. Rev.* **1964**, *135*, 1272.

Figure 3. The 2D azido-copper net and topology for (a) **2** and (b) **3**. Blue bonds stand for equatorial coordination, the dark red for axial coordination, and the light green line for topology analysis.

Cu^{II} ion. It appears that antiferromagnetic coupling would be expected for **1** for the *syn-syn* carboxylato bridge and the EO azido for a Cu-N-Cu angle of 126.8° .^{13a} Actually, in this situation, as Thompson et al. and Escuer et al. proposed, the countercomplementarity effect of the two ligands may explain the strong ferromagnetic coupling, not simply the sum of the two separated components.^{20,21}

The low-temperature magnetic measurements of **2** and **3** show spontaneous magnetization. At 300 K, the $\chi_m T$ product per Cu^{II} ion has a value of $0.59 \text{ cm}^3 \text{ K mol}^{-1}$ (Figure 5a) and $0.61 \text{ cm}^3 \text{ K mol}^{-1}$ (Figure 5b) for **2** and **3**, respectively, slightly above the expected $0.375 \text{ cm}^3 \text{ K mol}^{-1}$ for an isolated Cu^{II} ion with $S = 1/2$ and $g = 2.0$. As the temperature decreases, the $\chi_m T$ product increases steadily, until below

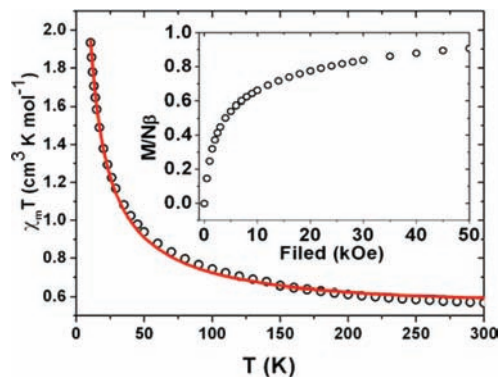
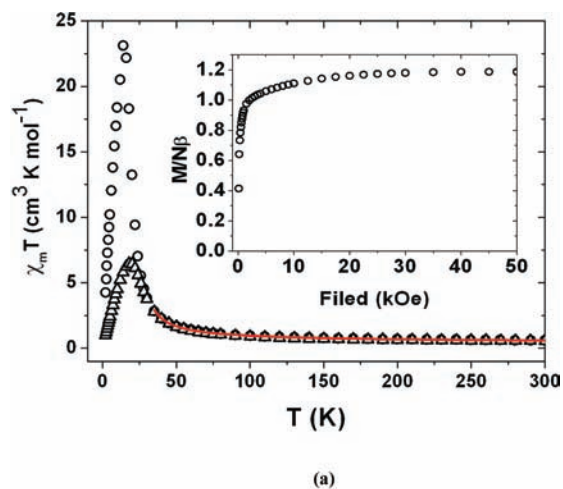
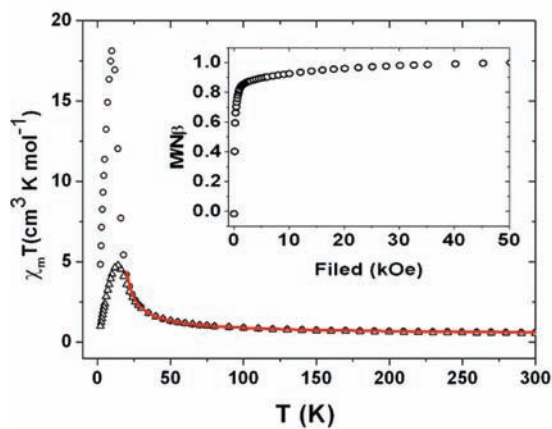


Figure 4. $\chi_m T$ vs T plot for **1** at 0.3 T applied field. The solid line is the best fit to the experimental data. Inset: the plot of the field dependence of the magnetization at 2 K.



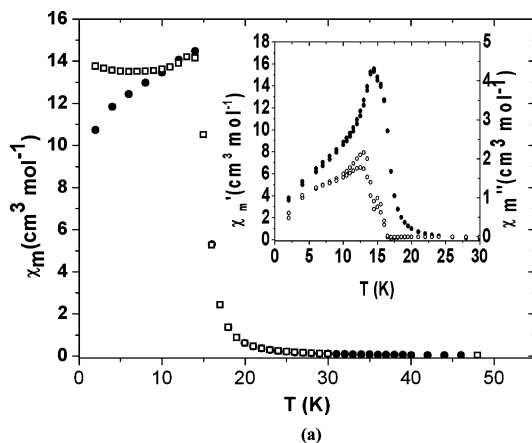
(a)



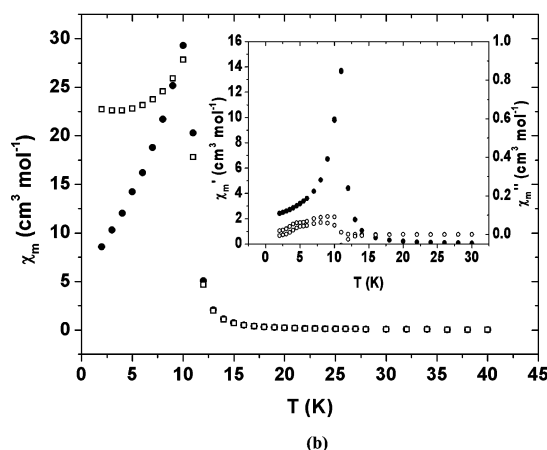
(b)

Figure 5. $\chi_m T$ vs T plot at 0.2 T (circles) and 1.0 T (triangles). The solid line is the best fit to the experimental data. Inset: Magnetization vs field plot at 2.0 K for (a) **2** and (b) **3**.

50 K, a pronounced rise is observed. A maximum value is reached at 14 K for **2** and 10 K for **3**. The magnitude of the maximum is strongly field-dependent. The susceptibility follows the Curie–Weiss law with $C = 0.49 \text{ emu mol}^{-1}$ and $\Theta = 53 \text{ K}$ down to 100 K for **2** (Figure S3, Supporting Information) and with $C = 0.53 \text{ emu mol}^{-1}$ and $\Theta = 43 \text{ K}$ down to 90 K for **3** (Figure S4, Supporting Information), suggesting strong ferromagnetic coupling between the Cu^{II} ions in **2** and **3**. On the basis of the magnetic structure



(a)



(b)

Figure 6. (a) Zero-field-cooled/field-cooled susceptibility plot for **2** at an applied field of 50 Oe (black squares, ZFC; white squares, FC). (b) Zero-field-cooled/field-cooled susceptibility plot for **3** at an applied field of 20 Oe (black squares, ZFC; white squares, FC). Inset: AC magnetic susceptibility plot with an oscillating AC field of 3.5 Oe at 1000 and 100 Hz. Black circles, in-phase susceptibility, χ_m' ; white circles, out-of-phase susceptibility, χ_m'' .

(discussed below), the intrachain coupling J^2 ($\hat{H} = -J\sum\hat{S}_i\hat{S}_i$) together with the mean field approximation²³ for interchain coupling zJ were used to fit the magnetic data of **2**, giving the best fit with parameters $g = 2.08$, $J = 93.10 \text{ cm}^{-1}$, $zJ = 3.40 \text{ cm}^{-1}$, and $R = 1.56 \times 10^{-4}$ ($R = \sum[(\chi_m T)_{\text{obsd}} - (\chi_m T)_{\text{calcd}}]^2 / \sum[(\chi_m T)_{\text{obsd}}]^2$) above 35 K (Figure 5a). The susceptibility of **3** above 25 K was simulated using the same model, giving a best fit with parameters $g = 2.23$, $J = 65.63 \text{ cm}^{-1}$, $zJ = 1.96 \text{ cm}^{-1}$, and $R = 3.18 \times 10^{-4}$ ($R = \sum[(\chi_m T)_{\text{obsd}} - (\chi_m T)_{\text{calcd}}]^2 / \sum[(\chi_m T)_{\text{obsd}}]^2$) (Figure 5b). The interchain interaction zJ was attributed to the interactions of chains in one layer and the interlayer coupling. However, the layers are well-separated, and the interactions between them are very small. Complexes **2** and **3** behave as 2D ordered magnets. A zero-field-cooled/field-cooled measurement shows spontaneous magnetization below 20 K for **2** (Figure 6a) and below 14 K for **3** (Figure 6b), indicating the onset of a ferromagnetic state. Furthermore, the magnetization versus field plot at 2 K shows spontaneous magnetization to a saturation value of 1.18, which indicates a ferromagnetically

(23) (a) Myers, B. E.; Berger, L.; Friedberg, S. A. *J. Appl. Phys.* **1969**, *40*, 1149. (b) O'Conner, C. J. *Prog. Inorg. Chem.* **1982**, *29*, 203.

ordered state at this temperature for **2** (Figure 5a inset). The magnetization versus field plot at 2 K of **3** also shows spontaneous magnetization to a saturation value of 0.99 per Cu^{II} ion, indicating a ferromagnetically ordered state (Figure 5b inset). AC magnetic susceptibility data were also collected for **2**. A strong out-of-phase signal appeared in the χ_m'' versus T plot at 13 K, as a decrease of the in-phase (χ_m') signal was observed (Figure 6a inset). The shape of the out-of-phase signal shows a sharp peak overlapping with a broader one, at lower temperatures, indicating the presence of more than one slow-relaxation phenomenon taking place below 13 K, which may be attributed to the moving of the domain wall that was frequent in the 2D structure.²⁴ For **3**, the AC magnetic susceptibility data show the appearance of a weak out-of-phase signal at 10 K, similarly to what was observed for **2**; the out-of-phase signal seems to have its origin in two different processes that are likely due to a small amount of impurity in the sample (Figure 6, inset).

In **2**, two distinct magnetic exchange pathways, in the two directions of the Cu^{II} layers, can be described: (i) Along the chains, the possible magnetic exchange pathways are provided by the *syn,syn*-carboxylato group and two end-on azido ligands bound to the $d_{x^2-y^2}$ orbitals of the Cu^{II} centers (with Cu–N distances of 1.98–2.01 Å and a Cu–N–Cu angle of 108.16°) and to the d_z^2 orbitals (Cu–N distances of 2.6–2.7 Å and a Cu–N–Cu angle of 75.09°). (ii) Perpendicular to the chains, end-to-end azido ligands mediate a weak ferromagnetic interaction between the magnetic $d_{x^2-y^2}$ orbital of one Cu^{II} and the full d_z^2 orbitals of the other Cu^{II} ions, which are mismatched for interaction through the azide. A priori, one might think that end-on azide ligands displaying large Cu–N–Cu angles like those in **2** should afford antiferromagnetic coupling, as calculated by Ruiz et al. for [Cu₂(EO-N₃)₂] planar units.^{13a} However, that is not the case in **2**. The magnetic orbital on each Cu^{II} center is $d_{x^2-y^2}$, which is not parallel but at a 64° canting angle (Figure 7a), resulting in the nonplanar [Cu₂(EO-N₃)₂] units. Furthermore, the second azido ligand is bound to the full axial d_z^2 orbitals of both Cu^{II}; thus, there is not an allowed superexchange pathway through this ligand. All of these result in weak ferromagnetic exchange, both inter- and intrachain.²⁵ This can explain the two features of the AC measurement: one corresponds to the ferromagnetic ordering in the lattice, while the weak interchain ferromagnetic interaction gives rise to the 2D soft ferromagnetic behavior of **2** and the second AC feature. However, there is no hysteresis at 2 K, due to the lack of three dimensional ordering in **2**, since the layers are not magnetically coupled (Figure S5, Supporting Information).

For **3**, the structure is very similar to that already discussed above for **2**, and the same magnetic exchange pathways are applied. The Cu^{II} ions in **3** are pentacoordinated in a square-pyramidal fashion, with a very elongated apical Cu–N distance of 2.726 Å, defining the z axis on the metal center.

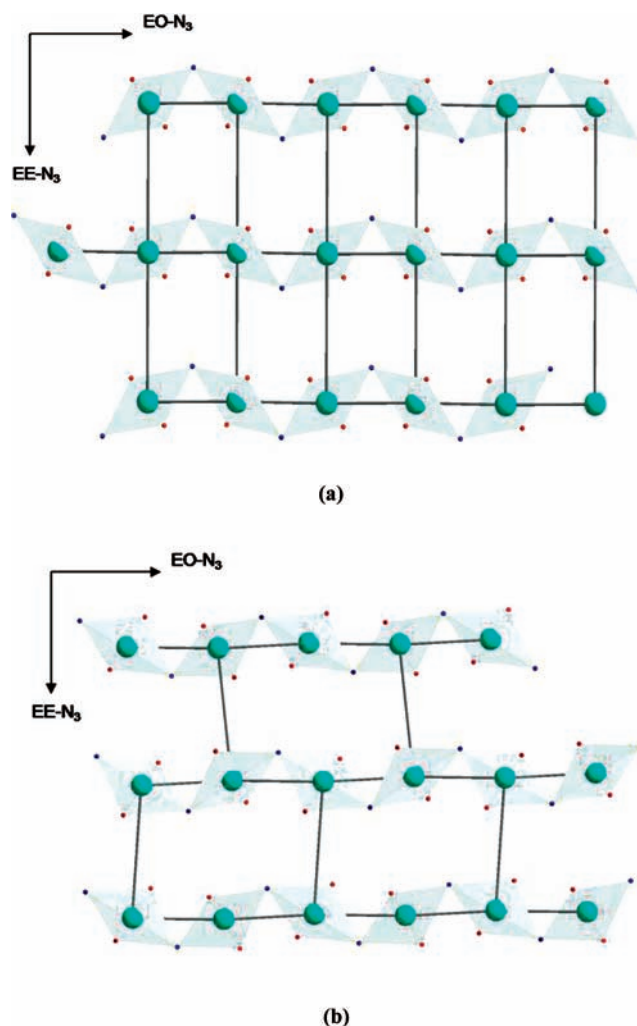


Figure 7. (a) View of **2** along the c direction of the unit cell (the Cu^{II} layers lay along the ab plane). The xy plane of the Cu^{II} centers are shown. (b) View of **3** along the a axis of the unit cell (the Cu^{II} layers lay along the bc plane). The xy planes on each Cu^{II} ion are shown.

Just like in **2**, there is ferromagnetic coupling along the chains of Cu^{II} ions bridged by a *syn,syn*-carboxylato group and an end-on azido ligand bound to the $d_{x^2-y^2}$ orbitals of the Cu centers (with Cu–N distances of 1.98–2.01 Å and a Cu–N–Cu angle of 116.85°). In **3**, the basal planes of the Cu^{II} centers are canted at a 59.84° angle (Figure 7). The chains are linked together to form layers via end-to-end azido ligands that provide a weak ferromagnetic exchange pathway by bridging full d_z^2 orbitals of one Cu^{II} to the half-full $d_{x^2-y^2}$ of the Cu^{II} in the neighboring chain. The situation is very similar to that in **2**, but in **3**, only half the exchange pathways exist since the Cu^{II} ions of **3** are pentacoordinated (Figure 7b). This fact is probably due to the steric bulk of the naphthyl group of the carboxylate and is most likely responsible for the fact that the ferromagnetic phase appears at lower temperatures for **3** than for **2**.

The big dihedral angle of the basal planes of the Cu^{II} centers, in **2** and **3**, as well as the countercomplementarity effect lead to the total ferromagnetic exchange in these complexes in spite of a big Cu–N–Cu angle. It will be noticed that the difference in J values of the chains in **1**, **2**, and **3** reflects the difference in the Cu–N–Cu angle. This

(24) (a) Coronado, E.; Galón-Mascarós, J. R.; Gómez-García, C. J.; Murcia-Martínez, A. *Chem. Eur. J.* **2006**, *12*, 3484. (b) Thétiot, F.; Sala-Pala, J.; Galón-Mascarós, J. R.; Golhen, S. *Chem. Commun.* **2002**, 1078.

(25) Colacio, E.; Costes, J.-P.; Domínguez-Vera, J. M.; Maimounac, I. B.; Suárez-Varela, J. *Chem. Commun.* **2005**, 534.

Table 3. Pertinent Cu–N–Cu Angles (deg) and Interactions for the Carboxylato/EO Azido Mixed-Bridged Copper Complex

Cu–N–Cu angles (deg)	J/cm^{-1}	ref
126.8	39	this work ¹
124.3	48	ref 17a
116.85	65.63	this work ³
116.09	69.7	ref 17b
111.9	75	ref 21
108.16	93.10	this work ²
107.6	126	ref 10a
106.7	80 ± 5	ref 15a
106.6	80	ref 17a
106.5	126	ref 10a
105.52	63	ref 10b
103	89	ref 17b

is consistent with a previously reported copper complex with carboxylato/EO-azido ligands. It is observed that the ferromagnetic coupling in the carboxylato/EO-azido Cu^{II} systems increases with the decrease of the Cu–N–Cu angle, with a maximum near 108°. The correlation is shown in Table 3—all of the superexchange parameters J correspond to two Cu ions bridged by one carboxylato and one EO-azido ligand. They were obtained using the Hamiltonian $\hat{H} = -J\sum_i \hat{S}_i \hat{S}_i$.

Conclusion

Three new azido–copper complexes with aromatic carboxylates as coligands have been structurally and magnetically characterized. The three complexes reported here, although having the same chemical formula, that is, [Cu(RCOO)(N₃)₂]_n, where R is in each case a different aromatic group, display very different solid-state structures and magnetic properties. Structural analyses show that

complex **1** is formed by isolated carboxylato/EO azido mixed-bridged chains, while **2** and **3** are 2D azido–copper networks displaying μ -(1,1,3,3) and μ -(1,1,3) azido coordination modes, respectively. The change of the structure depending on the R group of the carboxylate was clearly observed from X-ray analysis. Introducing steric bulk to the side of the benzoate adjusts the linkage of the azido anions and the coordination geometries of the metal center. Spontaneous resolution occurs in **2**, giving a chiral complex. The magnetic behavior of **1** is that of an isolated ferromagnetic chain. Complexes **2** and **3** are 2D magnets with transition temperatures of 13 and 10 K. These three complexes are good new examples of the azido-bridged copper complex family. We have shown here a good example of crystal engineering, in which the addition of substituents to a simple aromatic carboxylate alters the structure of the complexes obtained as well as allows the fine-tuning of their magnetic properties.

Acknowledgment. This work was financially supported by the 973 Program of China (2007CB815305), the NNSF of China (50673043 and 20773068), and NSF of Tianjin, China (07JCZDJC00500). E.C.S. acknowledges financial support from the Spanish Government (Grant CTQ2006/03949BQU and Juan de la Cierva fellowship).

Supporting Information Available: X-ray crystallographic data for complexes **1–3** in CIF format and Figures S1–S5. These materials are available free of charge via the Internet at <http://pubs.acs.org>.

IC802066A